Spectral Equilibration and Primary Photochemistry in *Heliobacillus mobilis* at Cryogenic Temperature

Ursula Liebl,[‡,§] Jean-Christophe Lambry,[‡] Jacques Breton,[§] Jean-Louis Martin,[‡] and Marten H. Vos*[,‡]

Laboratoire d'Optique Appliquée, INSERM U451, Ecole Polytechnique-ENSTA, 91761 Palaiseau Cedex, France, and SBE/DBCM, CEA Saclay, 91191 Gif-sur-Yvette Cedex, France

Received October 8, 1996; Revised Manuscript Received January 22, 1997[⊗]

ABSTRACT: We performed multicolor femtosecond transient absorption measurements on membranes of the photosynthetic bacterium *Heliobacillus mobilis* at 20 K, by selective excitation at either the red or the blue extreme of the bacteriochlorophyll *g* Q_Y band, which is split in three spectral forms (Bchl *g* 778, 793, and 808) at low temperature. In contrast to room temperature, there is no observable uphill energy transfer upon excitation at the red extreme. This provides a direct experimental confirmation of the expected strong temperature dependence of uphill energy transfer in multichromophore systems. Upon excitation at the blue edge, downhill energy transfer is observed on time ranges varying over 2 orders of magnitude and is discussed in terms of four distinct energy transfer processes: Bchl *g* 778* → Bchl *g* 793* (∼50 fs); Bchl *g* 778* → Bchl *g* 808* (∼400 fs); Bchl *g* 793* → Bchl *g* 808* (∼1.4 ps); and within Bchl *g* 808* (∼7 ps). Surprisingly, the amount of oxidized primary donor $P798^+$ formed on the time scale of picoseconds and tens of picoseconds was found to depend on the excitation conditions: trapping occurs mainly in ∼80 ps and slower from directly excited Bchl *g* 808* and can additionally occur in a few picoseconds from Bchl *g* 778* and Bchl *g* 793* upon blue excitation. This finding implies that spectral equilibration is not complete prior to charge separation and furthermore is inconsistent with a funnel model, in which P798 is surrounded by long-wavelength pigments. More generally, we discuss to what extent our data bring constraints on the spatial distribution of the different spectral forms of the pigments.

Photon energy captured by photosynthetic organisms is used for photochemistry with a very high quantum yield. Primary photochemistry occurs via a sequence of redox reactions amongst a few highly specialized (bacterio)chlorins bound to the reaction center (RC)[1] complex and is initiated by the population of the lowest excited state P* of the primary donor P, a dimer of (bacterio)chlorophylls. The bulk of the other (bacterio)chlorin pigments, which are located either on the RC complex or on separate antenna complexes, in a stoichiometry varying between organisms from ∼20−10000 per RC, serves to direct the excitation energy toward P. The Q_Y transitions of these pigments are distributed over different energies, due to variations in the pigment−pigment and pigment−protein interactions within the complexes. Generally, the P → P* transition is located in the low-energy part of the distribution. Upon white light illumination, the absorbed energy is transferred, by (generally overall downhill) excitation energy transfer amongst the pigments, toward a population of excited states in thermal equilibrium, a process termed spectral equilibration. At physiological temperatures, this population includes P*, a feature which is thought to be important for the high efficiency of primary photochemistry.

If thermal equilibrium has been reached, the lowest-lying excited state, corresponding to the red-most optical transition, has the highest probability to be occupied. Intuitively, in the optimal situation for a high quantum yield of radical pair formation, we should find no lower-lying states than P*. Interestingly, in most antenna−RC systems, this is far from being the case. For instance, long-wavelength transitions are present at 896 nm in the core (LH1) antenna complex of the purple bacterium *Rhodobacter sphaeroides* (where P absorbs at ∼860 nm) and at 808 nm in the RC of heliobacteria (where P absorbs at ∼798 nm). At room temperature, the energy difference between the lowest energy transition and P is not more than 1−2 *kT* (*k* being the Boltzmann factor and *T* the absolute temperature). Thus, as mentioned above, P* is thermally accessible from all excited states of the pigment complex. It has been argued that a few long-wavelength transitions can even increase the overall probability for an excitation to be on P* by reducing the effective number of excited states in (thermal) equilibrium with P* (Trissl, 1993).

At cryogenic temperatures, a different situation applies. At 20 K, $kT = 16\ cm^{-1}$, which corresponds to a difference of ∼1 nm for optical transitions near 800 nm. Therefore, if thermal equilibration is reached prior to charge separation, this would suggest that P* can only be formed at a very low rate and the radical pair yield should decrease. For instance, if we assume a rate of electron transfer from P* of $(2\ ps)^{-1}$, a 2 ns intrinsic excited state lifetime and a 160 cm^{-1} (10*kT*) energy gap between P* and the excited state of the long-wavelength pigment(s), then we find a yield of only 5% for the case that there is only one such pigment and even less if there are more (as seems to be the case in many complexes).

‡ Ecole Polytechnique-ENSTA.
§ CEA Saclay.
⊗ Abstract published in *Advance ACS Abstracts,* May 1, 1997.
[1] Abbreviations: Bchl, bacteriochlorophyll; DAS, decay associated spectrum; EDTA, ethylenediaminetetraacetic acid; fwhm, full-width at half-maximum; MOPS, 3-(*N*-morpholino)propanesulfonic acid; PMS; *N*-methyldibenzopyrazine methosulfate; PS; photosystem; RC, reaction center; SVD, singular value decomposition.

S0006-2960(96)02519-6 CCC: $14.00

Indeed, at 6 K, a reduced yield of charge separation, as measured on the millisecond time scale, has been reported for chromatophores of *Rhodopseudomonas viridis* (45%) and *Heliobacterium chlorum* (70%) (Kleinherenbrink et al., 1992). These values are still surprisingly high if one takes into account the spectral shifts between the absorption maxima of P and the long-wavelength pigments in the antenna. Accordingly, Lin et al. (1994b) were unable to simulate the low-temperature trapping kinetics in *Heliobacillus mobilis* using a Boltzmann-type model. Kleinherenbrink et al. (1992) and Lin et al. (1994b) pointed out that in chromatophores the position of the 0-0 transition of P is unknown and might be located substantially more to the red than the maximum of its photobleaching. They suggested that this could explain the apparent high rate of energy transfer from long-wavelength antenna pigments to P. Kleinherenbrink et al. (1992) also found that the yield of charge separation was independent of the excitation wavelength and suggested that spectral equilibration occurs prior to charge separation, also at cryogenic temperatures. Further studies using picosecond one-color spectroscopy (van Noort et al., 1994) and femtosecond multicolor spectroscopy under nonselective excitation (Lin et al., 1994b) were also supporting this view. However, direct measurements of spectral equilibration at cryogenic temperatures and an experimental assessment of the presumed very low rate of uphill energy transfer have not yet been reported. Unambiguous discrimination between spectral equilibration and other processes, such as charge separation, occurring on the femtosecond and picosecond time scales requires multicolor femtosecond spectroscopy under *selective* excitation. Using this technique, the present work aims at elucidating the pathways and kinetics of energy transfer and trapping in *H. mobilis* at cryogenic temperature. It will be shown that equilibration actually occurs on a range of time scales spanning tens of femtoseconds to several picoseconds and that kinetics of radical pair formation are excitation wavelength dependant, even on the time scale of tens of picoseconds.

Energy transfer has been studied recently under selective excitation conditions in a number of isolated photosynthetic pigment−protein complexes with known structure, including the bacterial reaction center (Haran et al. 1996; Stanley et al. 1996; Jonas et al. 1996; Vos et al., 1996), the light harvesting 2 complex (Hess et al., 1995; Monshouwer et al.; 1995; Jimenez et al., 1996), and the FMO complex (Savikhin & Struve, 1994). For the RC core of photosystem I (PS I), which is more closely related to the RC of heliobacteria (see below), the structure has been partially resolved and the position of part of the ∼100 cofactors has been modeled (Krauss et al., 1993; Fromme et al., 1996). Femtosecond studies of PS I with selective excitation in the chlorophyll *a* Q_Y band have thus far only proven possible in a variety of detergent-isolated particles containing different numbers of pigments per complex (Du et al., 1993; Hastings et al., 1995; White et al., 1996). No such studies have been performed at low temperature.

Heliobacteria are unique in that all energy transfer and primary electron transfer occurs in a single bacteriochlorophyll-containing protein complex, called reaction center−antenna complex (RC) [for reviews, see Amesz (1995), Blankenship (1994), and van Grondelle et al. (1994)]. This complex can be studied directly in membrane fragments. The general photochemistry is thought to be similar to that of PS I and of green sulfur bacteria, both of which are connected to larger antenna proteins *in vivo*. The RC core of heliobacteria is a homodimer (Liebl et al., 1993) and binds bacteriochlorophyll (Bchl) *g*, a type of Bchl found only in heliobacteria (Brockmann & Lipinski, 1983) in a stoichiometry of 35−65 molecules of Bchl *g* per RC, estimated using a variety of methods (Vos et al., 1989; Trost & Blankenship, 1989; van de Meent et al., 1990, 1991; Deinum, 1991). Primary electron transfer occurs directly [Liebl et al., 1996; see also Lin et al. (1994a)] from the primary donor P798, a dimer of Bchl *g* or *g*′ (van de Meent et al., 1990), to the primary acceptor A_0, identified as 8′-hydroxychlorophyll *a* (van de Meent et al., 1991). At room temperature, the overall process of energy transfer to P798 and charge separation occurs on the time scale of 5−30 ps (Trost & Blankenship, 1989; van Noort et al.; 1992, Lin et al., 1994a, Liebl et al., 1996) whereas spectral equilibration mainly occurs in the time range of ∼100−500 fs for both uphill and downhill energy transfer, and probably also to some extent on the picoseconds time scale (Liebl et al., 1996).

The inhomogeneously broadened, ∼40 nm wide Bchl *g* Q_Y band of the RC complex has a maximum at 788 nm and is featureless at room temperature. Also, in studies at room temperature on spectral equilibration, no features can be assigned to specific pigment pools (Lin et al. 1994a; Liebl et al., 1996). By contrast, the low-temperature absorption spectrum is clearly structured, and this has led to the assignment of three different pools of transitions (van Dorssen et al., 1985), labeled Bchl *g* 778, 793, and 808 from the peaks in the second-derivative spectrum. Circular dichroism spectroscopy has indicated that significant excitonic coupling only plays a role within the Bchl *g* 793 band, which was suggested to be composed of two close-lying coupled bands (van Dorssen et al., 1985). Therefore, as will be done in this paper, the spectroscopically distinct transitions can be discussed in terms of pools of pigments, possibly including dimers in the case of Bchl *g* 793. While the origin of the spectroscopic clustering of the pigments in distinct pools rather than a more continuous spectral distribution (as well as the homogeneous width of the transitions) is unknown, it will prove convenient to discuss the spectral evolution at low temperature in terms of these pools. It is interesting to note that in isolated PS I preparations (Shiozawa et al., 1974, van der Lee et al., 1993) and in core preparations of green sulfur bacteria [see, for instance, Vasmel et al. (1983)] separate pools are also distinguished at low temperature. Previous spectral equilibration studies in *H. mobilis* at room temperature (Liebl et al., 1996) and simulations of the trapping process at low temperature (Lin et al., 1994b) indicate that the spectroscopically distinct pigments are not related to spatially distinct clusters; yet, there is no clear proof of this. In this context, the spectral equilibration studies in heliobacteria at low temperature described in the present paper are particularly interesting in view of the spectroscopic resolution of distinct pools. They should allow to obtain more precise information on the pigment organization, relevant for our understanding of the functioning of the complex at physiological temperatures.

MATERIALS AND METHODS

Membranes of *H. mobilis* were prepared as described by Liebl et al. (1990). All buffers were degassed and stored under argon. A washing step of the membrane fraction in

20 mM MOPS, pH 7.0, containing 1 mM EDTA, was added. The pelleted membrane fragments were resuspended in a mixture of the above buffer and glycerol (50/50 v/v) to an optical density of ~1.0 (optical path length 1 mm) at 788 nm. Sodium ascorbate (20 mM) and PMS (10 μM) were added. Measurements were performed at 20 K on a sample in a Plexiglas cell (optical path-length 1 mm) cooled in the dark using a convection cryostat.

The femtosecond spectrometer, operating at 30 Hz, was used in a configuration described previously (Liebl et al., 1996) with pump pulses centered at either 770 nm (30 fs fwhm) or 812 nm (60 fs fwhm) and a continuum probe pulse that was essentially chirp-free (<10 fs) over the wavelength range 770−830 nm. Unless stated otherwise, the pump and probe beams were polarized at magic angle (54.7°) using Polarcor polarizers. The intensity of the pump beam was adjusted so that after 1 ps less than 0.8% of the Q_Y band surface was bleached. In this regime, all signals were found to be linear with excitation intensity.

Data were taken in two different scan types: 1 ps full scale and 4/50 ps double time scale. During each scan, 30 shots were averaged at each time delay and approximately 50 scans were averaged for each data set, so that for each data set on the order of 10^5 pulse pairs illuminated the same sample volume. Due to these conditions, a considerable fraction of P798, which may be as high as 50% (Nitschke et al., 1990), is probably permanently in the oxidized state. Flash-formed triplet states decay in the nanosecond time scale (Kleinherenbrink et al., 1991) and are not expected to be present prior to the flash.

In the 770−830 nm region, the results were analyzed in terms of exponential functions using singular value decomposition [SVD, see Press et al. (1989)] as described previously (Liebl et al., 1996).

RESULTS

Transient absorption spectra in the Bchl *g* Q_Y region were collected with excitation pulses centered either at 812 nm or at 770 nm (Figure 1A). For all data shown, the pump and probe pulses were polarized at magic angle. In this way, an isotropic population is probed and the results under both conditions can be directly compared.

Excitation at 812 nm. The 812 nm pump pulse spectrally overlaps only with the absorption spectrum of the red-most pigments. Upon excitation at 812 nm, a narrow (~8 nm fwhm) bleaching (maximum at 810 nm) appears instantaneously (Figure 1B), corresponding approximately to the shape of the pump pulse weighted by the absorption spectrum. The spectrum evolves little on the time scale up to a few picoseconds. This contrasts with the same experiment at room temperature (Liebl et al., 1996), where a blue shift in ~300 fs of the initial bleaching reflecting uphill energy transfer was observed. Our present observation is in agreement with the notion, that at 20 K, no significant uphill energy transfer can occur and that upon excitation of the lowest energy transitions the distribution of initially created excited states is approximately in thermal equilibrium.

After 3.5 ps, the maximum of the bleaching is at 811 nm. This small red-shift, which mainly takes place on the time scale of ~100 fs (see Figure 2A for subpicosecond kinetics at individual wavelengths) may be due either to some

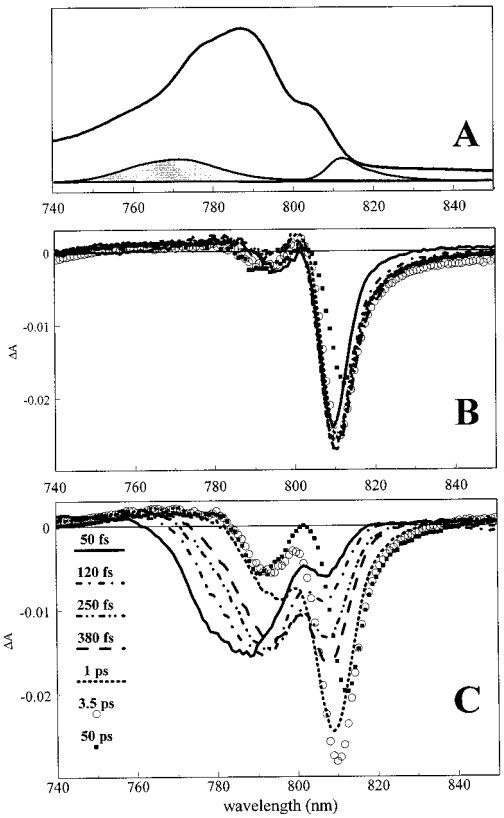

FIGURE 1: Ground state (A) and transient absorption spectra at selected delay times from 50 fs to 50 ps in the Bchl *g* Q_Y band region upon excitation at 812 nm (B) and 770 nm (C). Hatched curves in (A): spectral profiles of the respective excitation pulses.

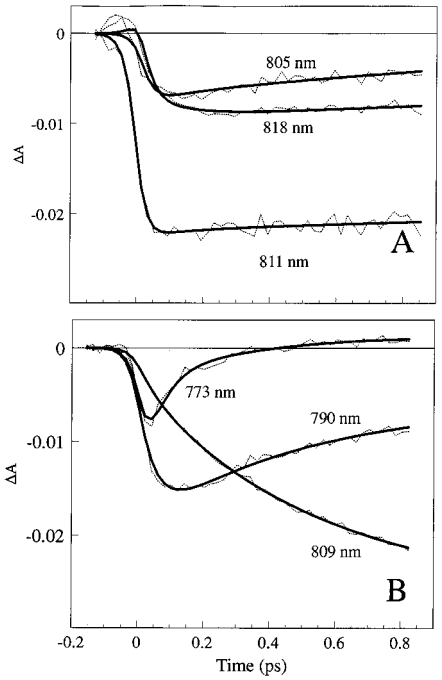

FIGURE 2: Subpicosecond kinetics (···) at selected wavelengths upon excitation at 812 nm (A) and 770 nm (B). Exponential fits (—) with time constants from the global analysis as described in the text.

downhill energy transfer leading to bleaching of yet more red-lying transitions or to nuclear dynamics within the initially created excited states leading to red-shifting of the (stimulated) emission. During the first few picoseconds, only a very small bleaching is observed around 793 nm, where

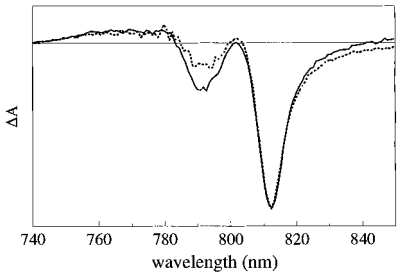

FIGURE 3: Transient absorption spectra at $t = 50$ ps upon excitation at 812 nm (···) and 770 nm (—). Data taken from Figure 1 and normalized at 812 nm.

the primary donor P798 absorbs at low temperature (Smit et al., 1989).

Excitation at 770 nm. The 770 nm pulse overlaps with the blue side of the spectrum and excites predominantly the transitions of the Bchl *g* 778 pool. Upon excitation at 770 nm, a bleach centered at ~785 nm appears instantaneously (Figure 1C). In contrast to red-wing pumping, under these conditions a pronounced spectral evolution takes place during the first few picoseconds. The initially broad (~25 nm fwhm) bleaching shifts to the red and eventually distributes among two narrower bands centered near ~810 and ~790 nm. The shift occurs in several phases as can be clearly seen in the kinetics at individual wavelengths (Figure 2B). The initial bleaching in the 770 nm region disappears in a few hundred femtoseconds, whereas the rise of the signal around 810 nm also contains slower components.

After 3.5 ps, the relative bleach around 793 nm is much stronger upon excitation at 770 nm than upon excitation at 812 nm. This indicates that, upon excitation at 770 nm, either significant charge separation takes place within a few picoseconds or energy transfer from Bchl *g* 793 to Bchl *g* 808 occurs partially on a time scale slower than a few picoseconds. For both excitation conditions, the bleaching around 810 nm decays (partially) on the time scale of tens of picoseconds. Concomitantly, there is a modest increase in the bleaching near 790 nm, where P798 absorbs, indicating that some P798 oxidation occurs on this time scale. The decay of the bleach near 810 nm may also be due to additional Bchl *g** decay to the ground state, directly or via trapping by $P798^+$ in RCs where $P798^+$ is present prior to excitation (see Discussion).

Finally, anisotropy measurements under 770 nm excitation (not shown) yielded a rough estimate of 300 fs for the average single step energy transfer between isoenergetic Bchl *g* 778 and 793 pigments. This is in the same time range as the values found for room temperature (Liebl et al., 1996).

Comparison of Two Excitation Conditions at "Long" Times. A remarkable finding is that the transient spectra under the two excitation conditions are dissimilar even after several tens of picoseconds. In view of the possibility of a preparation-dependent steady state $P798^+$ concentration (see below), we explicitly note that these results were sample independent. Figure 3 directly compares the transient spectra at $t = 50$ ps. The relative amplitude of the bleach near 793 nm is still more than 50% higher with 770 nm excitation than with 812 nm excitation. This shows that the net rate of charge separation depends on the excitation conditions, which implies that spectral equilibration is not completed prior to charge separation.

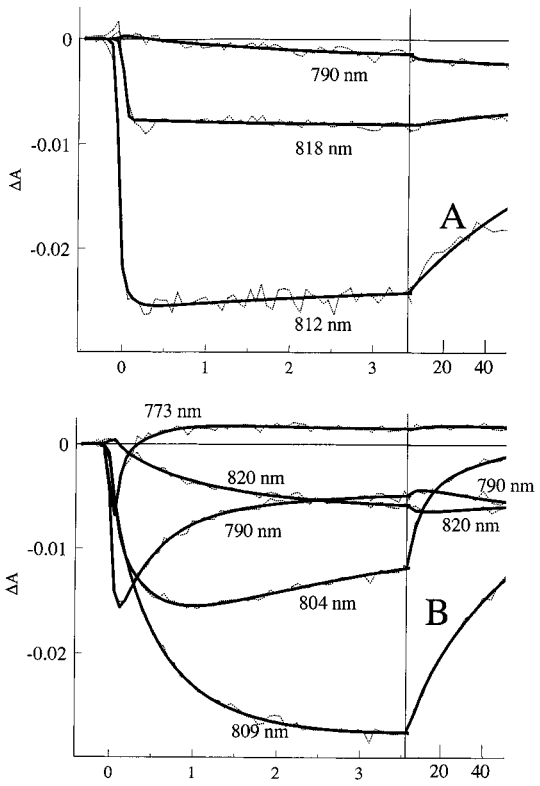

FIGURE 4: Kinetics on the 4 and 50 ps time scales (···) at selected wavelengths upon excitation at 812 nm (A) and 770 nm (B). Exponential fits (—) with time constants from the global analysis as described in the text.

Figure 4 shows the kinetics at individual wavelengths on a dual (4 and 50 ps) time scale. They highlight the very complex spectral evolution, especially upon excitation at the blue side of the absorption band.

Data Analysis. For both excitation conditions, an SVD analysis was performed on the data sets using only the essentially chirp-free spectral range (770−830 nm). Subsequently, the kinetics of the SVD components, which deviate significantly from zero (three for the 1 ps scans and four for the 4/50 ps scans), were fit with exponential functions. For each excitation condition, the minimal number of exponentials needed to satisfactorily fit the ensemble of these SVD components for the different scan times (1, 4, and 50 ps full scale) was determined iteratively. For the 812 nm data, three exponentials were needed, whereas for the 770 nm data, as many as five exponentials were needed. The decay associated spectra (DAS) of the different exponential components, constructed from this analysis as described by Liebl et al. (1996), are shown in Figure 5.

With 812 nm excitation, the sub-10 ps components have time constants of 110 fs and 2 ps and are small with respect to the total signal and with respect to the sub-10 ps components found for 770 nm excitation. The 110 fs component corresponds to a red shift (isosbestic point 808 nm) of the main initial bleaching at 810 nm and is further associated with the disappearance of a very small initial bleaching around 790 nm. The 2 ps component has a positive contribution at ~790 nm and a negative contribution at ~805 nm, an indication that charge separation occurs to some extent on this time scale. The very small positive contribution at ~812 nm may indicate that some excitation equilibration by downhill energy transfer also occurs on the time scale of ~2 ps.

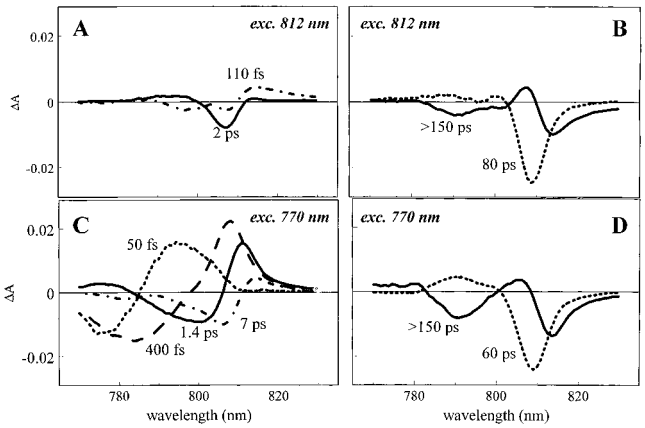

FIGURE 5: Decay-associated spectra in the Bchl *g* Q_Y band region upon excitation at 812 nm (A,B) and 770 nm (C,D).

With 770 nm excitation, a minimum of four sub-10 ps components is needed to describe the spectral evolution. Each exponential component is associated with a spectral red shift of the bleaching, characteristic for downhill energy transfer. The isosbestic points of the red-shifts are respectively at 785 nm (50 fs), 797 nm (400 fs), 806 nm (1.4 ps), and 810 nm (7 ps). As such components are not observed under excitation at 812 nm, they presumably reflect downhill energy transfer. The 50 fs component does not contribute at $\lambda > 810$ nm, showing that Bchl *g* 808 is not involved in this component. The other three components all have positive contributions at $\lambda > 810$ nm, indicating that they reflect, at least partially, energy transfer to (and within) Bchl *g* 808. At $\lambda < 785$ nm, only the 50 fs and 400 fs components contribute, indicating that energy transfer from Bchl *g* 778 occurs within a few hundred femtoseconds. The assignment of the components in terms of Bchl *g* pools will be discussed in more detail in the Discussion.

On the time scale longer than 10 ps, an additional fit component was found, spectrally characterized by negative contributions near ~810 nm and positive contributions near ~790 nm, with optimal values for the time constants of 60 ps (770 nm excitation) and 80 ps (812 nm excitation). The time constant corresponds approximately to the ~70 ps component assigned to charge separation upon nonselective excitation by Lin et al. (1994b). The DAS of the long-time asymptotic spectrum (indicated ">150 ps" in Figure 5) still contains a considerable bleach around 812 nm (relatively more important for 812 nm excitation). This indicates that a significant fraction of Bchl *g* 808* does not decay on the ~100 ps time scale. Consistent with this, additional decay components with time constants >150 ps can be inferred from preliminary experiments on the 0−200 ps time domain (data not shown).

The bleaching near 790 nm in the time range of tens of picoseconds presumably reflects $P798^+$ formation. It is interesting to compare our data in this time range with the spectra reported by Lin et al. (1994b), from experiments associating low temperature (20 K) and isotropic detection (magic angle) with nonselective excitation at 590 nm. Even at delay times of tens of picoseconds, these spectra display a significantly higher ΔA790:ΔA810 ratio than our spectra (approximately 3 times larger than with excitation at 770 nm in the present experiments). This indicates that a larger amount of $P798^+$ is formed under their conditions. Several explanations can be offered for this difference. First, in contrast to either of our excitation conditions, the use of a pump pulse centered at 590 nm leads to direct excitation of P798 and close-lying isoenergetic pigments, which may lead to charge separation prior to spectral equilibration (see Discussion). In addition, there is a possibility that in our preparations a higher percentage of steady-state $P798^+$ is present. Indeed an indication that steady state $P798^+$ is present in our experiments comes from preliminary experiments at 670 nm, where the primary acceptor A_0 absorbs. Even after 200 ps the bleaching in the A_0 band was found to be much smaller than at room temperature. Earlier studies on *H. chlorum* membranes (Nitschke et al., 1990) have shown that illumination at 5 K results in the irreversible formation of $P798^+FeS^-$ (where FeS is an iron-sulfur cluster type F_A or F_B) in a fraction of the reaction centers, with a quantum yield of 3%. Under our experimental conditions of signal averaging on the same sample volume (see Materials and Methods), this fraction can be considered to be saturated with $P798^+$ and therefore the amount of steady state $P798^+$ independent of the excitation conditions. The fraction of the centers in which $P798^+$ is thus irreversibly formed [as high as 50% in the study reported by Nitschke et al. (1990)] may vary between different preparations and presumably correlates with the integrity of the FeS clusters (W. Nitschke, personal communication).

DISCUSSION

No Uphill Energy Transfer at Low Temperature. The present results using selective excitation of the different pigments give insight in the pathways and kinetics of energy transfer between the spectrally different pigments. Spectral equilibration generally involves both downhill and uphill energy transfer. Previous femtosecond transient absorption experiments under *selective* excitation at either edge of the Bchl Q_Y band have demonstrated that both processes indeed occur at room temperature in a few hundred femtoseconds in *H. mobilis* (Liebl et al., 1996), as compared to a few picoseconds in photosystem I (Hastings et al., 1995).

At *room* temperature, uphill energy transfer brings the system in an electronic excited state, which may be energetically higher than the energy of the initially absorbed photon, by extracting energy from the protein thermal bath. Macroscopically, if the initially populated distribution of excited states is "cold" (and the entropy low) with respect to the Boltzmann distribution of coupled excited states at the ambient temperature, then net uphill energy transfer occurs. By contrast, the present work demonstrates, in a direct experiment, that uphill energy transfer does not occur at *cryogenic* temperature. As mentioned previously, *kT* at 20 K corresponds to a difference of 1 nm only for optical transitions near 800 nm. As this is much smaller than the homogeneous width of the absorption of the pigments and the (necessarily large) spectral width of the excitation pulses, spectral equilibration through detectable uphill energy transfer is indeed not expected to occur. To our knowledge, our results constitute the first direct experimental illustration in a multichromophore system of this expected and physically simple temperature effect on the uphill energy transfer component in spectral equilibration.

Downhill Energy Transfer. In contrast to excitation at the red edge of the Q_Y absorption band, a strong red-shift of the photoinduced bleaching occurs on the femtosecond and

picosecond time scales upon excitation at the blue edge, reflecting downhill energy transfer. We have shown previously (Liebl et al., 1996) that at room temperature downhill energy transfer between the ensemble of spectroscopically different pigments can be described by only two components of 100 and 500 fs. The present work reveals downhill energy transfer over a much wider time range at 20 K, that is described by as many as four components ranging from 50 fs to 7 ps. As it will be shown below, these can be described in terms of transfer between the different pigment pools which are spectroscopically distinguishable at low temperature.

Before discussing the spectral evolution in detail, we note that Bchl *g** − Bchl *g* difference spectra are composed of several elements: bleaching of the ground state transitions (GSB), appearance of excited state absorption (ESA), and stimulated emission (SE). As the overall signal is dominated by negative absorption changes, ESA will be ignored in the following discussion. SE will be spectroscopically apparent as an additional bleaching. At very short delay times, when nuclear motion on the excited state potential energy surface has not yet occurred, its spectrum will be close to that of the GSB. At longer delay times, it will shift, in the absence of uphill energy transfer overall to the red, and after spectral equilibration and vibrational relaxation the spectral shape of SE is expected to be close to that of the steady state spontaneous emission. The fluorescence spectrum of *H. chlorum* at 4 K has a maximum at 819 nm (van Dorssen et al., 1985) and presumably originates predominantly from the red-most pigments. Thus, the Stokes shift associated with the Bchl *g* 808 pigments can be estimated roughly at 10 nm. A small shoulder in the bleaching is indeed observed near ∼820 nm upon excitation at 812 nm at all delay times >50 fs and upon excitation at 770 nm at delay times >∼1 ps (Figure 1B,C). As the ground state does not absorb at ∼820 nm, we can unambiguously assign this signal to SE and conclude that stimulated emission contributes weakly to the signal. For the signal originating from the excited states of the more blue-absorbing pigments, populated at early delay times upon excitation at 770 nm, this is probably also the case. Therefore, the bleaching signal corresponding to excited states of a pigment pool is expected to be somewhat extended to the red compared to the corresponding ground state absorption.

The structure in the low temperature ground state Q_Y absorption band has led van Dorssen et al. (1985) to propose that at least three different pools are present, labeled Bchl *g* 778, 793, and 808. For comparison with the DAS of the components reflecting downhill energy transfer, we have decomposed the band (Figure 6A) into four Gaussian bands (maxima at 765, 781, 793, and 806 nm) in a way similar to that described by Smit et al. (1989) for *H. chlorum*. In the following, we will discuss the data in terms of the three mentioned pools. Although our deconvolution yields maxima of the bands which differ slightly from those proposed by van Dorssen et al. (1985) for *H. chlorum*, for convenience we will use the same nomenclature. The blue-most absorption (maximum of the broad deconvoluted band 765 nm) does not contribute to the bleaching in our experiments, and its origin remains unclear.

The 50 fs component has the shape of a spectral shift and seems to reflect energy transfer from at least the blue-most part of the Bchl *g* 778 pool to the Bchl *g* 793 pool. It is also possible that a spectral shift of the emission band, due to nuclear motion *within* Bchl *g* 778*, contributes to this component. However, as such shifts are small for direct excitation of Bchl *g* 808 in the case of 812 nm excitation, it is unlikely that such a spectral evolution would dominate the strong 50 fs component observed upon excitation of the more blue-absorbing pigments. Therefore, this component is mainly ascribed to energy transfer to the Bchl *g* 793 pool.

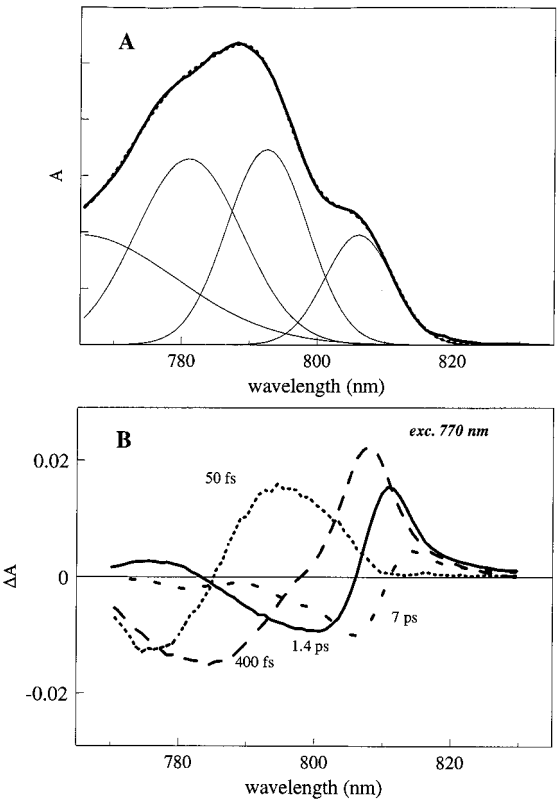

FIGURE 6: (A) Deconvolution of the Q_Y absorption band into four Gaussian bands with maxima at 764, 781, 793, and 806 nm. (B) Decay-associated spectra of the sub-10 ps components under excitation at 770 nm. Redrawn from Figure 5.

The 400 fs component clearly reflects energy transfer from the Bchl *g* 778 pool to the (red-most part of the) Bchl *g* 808 pool. Possibly, Bchl *g* 793* → Bchl *g* 808* energy transfer also contributes to a minor extent. After ∼1 ps, no further bleaching is observed at wavelengths below ∼780 nm (Figure 1), showing that all energy transfer from excited Bchl *g* 778 pigments is contained in the 50 fs and 400 fs components.

Consequently, the 1.4 ps component reflects energy transfer from the Bchl *g* 793 pool to the (red-most pigments of the) Bchl *g* 808 pool. In contrast to the situation described above for the Bchl *g* 778* depletion, the 1.4 ps component does not deplete the bleaching around 790 nm (Figure 1C, 3.5 ps). The shape of the remaining band around 790 nm is much like that at longer times, under both 770 and 812 nm excitation (Figure 3). Therefore, as will be discussed in detail in the following section, this remaining bleaching is most likely due to bleaching of the primary donor P798, which has a maximum at ∼793 nm at low temperature (Smit et al., 1989), rather than to some remaining excited Bchl *g* 793.

Finally, the 7 ps component with the isosbestic point at 810 nm most likely mainly reflects energy transfer within the heterogeneous Bchl *g* 808 pool, as also has been observed by Lin et al. (1994b).

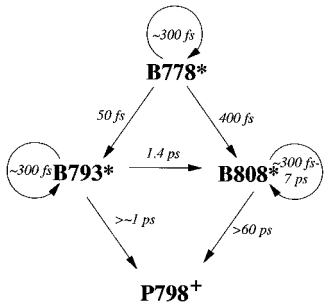

FIGURE 7: Scheme of energy transfer between the different bacteriochlorophyll *g* pools and trapping by P798 at 20 K. B778, B793, and B808 denote Bchl *g* 778, 793, and 808, respectively. The circular arrows refer to energy transfer within individual pigments of the same pool. For Bchl *g* 808 this arrow includes equilibration toward the most red-lying pigments.

It must be kept in mind that the spectroscopically distinct pools each correspond to a group of transitions of Bchl *g* pigments, each of which has a different interaction with the other pigments. Therefore, the rate constants deduced from this analysis should be regarded as averages of the rates for the pathways of energy transfer from the ensemble of initially populated excited states. Nevertheless, the analysis shows that downhill energy transfer can be described to first order with a relatively simple scheme in terms of the three different spectroscopically distinct pools as shown in Figure 7. Bchl *g* 778* is depleted by transfer to Bchl *g* 808* in ~400 fs and approximately 8 times faster (50 fs) to Bchl *g* 793*. These times can be attributed to those of single steps, as the anisotropy decay measurements indicate that energy transfer between the different Bchl *g* 778 molecules occurs roughly on the same time scale.

In our earlier room temperature experiments (Liebl et al., 1996), we found that Bchl *g* 778* → Bchl *g* 793*, Bchl *g* 778* → Bchl *g* 808* transfer, and transfer between isochromic pigments all take place in the 100−500 fs time domain with less well-separated spectral contributions of the different pools, which is generally consistent with a spatially heterogeneous distribution of the spectrally different pigments. The spectral separation at low temperature may allow to verify this for the different pools. In the following, we will compare the ratio of the rates for Bchl *g* 778* → Bchl *g* 793*and Bchl *g* 778* → Bchl *g* 808* transfer at 20 K with a rough estimate from the spectral deconvolution.

Electronic energy transfer between two pigments depends on the relative distance and orientation of the two pigments and, linearly, on the spectral overlap between the normalized emission spectrum of the donor and absorption spectrum of the acceptor. This is the case both for a dipole−dipole mechanism (Förster, 1948) and for an electron exchange mechanism (Dexter, 1952).[2] We assume the absorption bands of the individual pigments to be those of the deconvoluted bands (Figure 6A) and the corresponding emission bands to have the same Gaussian spectral shape, Stokes-shifted by 10 nm. As we cannot account for any possible inhomogeneous broadening of Bchl *g* in a protein matrix at 20 K, this estimation is necessarily crude [similar estimations were used in discussing energy transfer in PS I-type RCs by Causgrove et al. (1989) and Kleinherenbrink et al., (1992)]. We calculate, using a formula derived by Jean et al. (1988), that the spectral overlap ($\int A(\nu)F(\nu)\,d\nu$, in which A and F are the normalized absorption and emission as a function of frequency ν] between Bchl *g* 778 emission and Bchl *g* 793 absorption is 3−4 times higher than the spectral overlap between Bchl *g* 778 emission and Bchl *g* 808 absorption. Further, we estimate from the surface of the spectrally deconvoluted bands (Figure 6) that there are approximately 2 times more Bchl *g* 793 pigments than Bchl *g* 808 pigments. Taken together, the differences in spectral overlap and in pigment content correspond well with the factor of ~8 found for the ratio of the averaged rates. Whereas, in view of the assumptions used in this comparison, the extreme closeness of this correspondence is probably fortuitous, it shows that this analysis is consistent with an arrangement in which the average relative distance and orientation between Bchl *g* 778 and Bchl *g* 793 pigments is similar to that between Bchl *g* 778 and Bchl *g* 808 pigments. In line with our room temperature findings, this would imply that the pools of pigments are not organized in a sequential way and that at least the Bchl *g* 778 pigments are heterogeneously distributed with the other pigments. This reasoning does not include the relative spatial distribution of the Bchl *g* 793 and Bchl *g* 808 pigments, which may be less heterogeneous as discussed below.

Apparently, in contrast to the situation at room temperature (Liebl et al., 1996), the direct Bchl *g* 778* → Bchl *g* 808* transfer does not contain very fast (~100 fs) components at 20 K. This is probably the consequence of a diminished spectral overlap at low temperature.

Part of the ~400 fs Bchl *g* 778* → Bchl *g* 808* transfer may proceed via Bchl *g* 793* if the latter is very short-lived. Additionally, some Bchl *g* 793* → Bchl *g* 808* transfer may be contained in the 400 fs component. However, at least a considerable part of the Bchl *g* 793* → Bchl *g* 808* transfer occurs in ~1.4 ps. This is much slower than the ~50 fs Bchl *g* 778* → Bchl *g* 793* transfer, whereas the spectral overlaps for both transfers, estimated as above, are similar, and probably even less favorable for Bchl *g* 778* → Bchl *g* 793* transfer if the bands are substantially inhomogeneously broadened.[3] This indicates that at least some of the Bchl *g* 793 pigments are located somewhat further away from the Bchl *g* 808 pigments (or oriented less favorably for energy transfer) than from the Bchl *g* 778 pigments. Furthermore, the 1.4 ps Bchl *g* 793* → Bchl *g* 808* transfer time is considerably slower than the average transfer time of ~300 fs for isochromic pigments. Therefore, it is possible that BChl *g* 793 is spatially organized to a certain extent in clusters in which excitations equilibrate before being transferred to Bchl *g* 808. This possibility is discussed below in the context of the spatial position of P798.

Yield of Charge Separation and Location of P798. Lin et al. (1994b) interpreted the 70 ps component from their analysis as the only component reflecting $P798^+$ formation at 20 K, although their data obtained upon nonselective excitation display significant bleaching around 790 nm at

[2] The definition of the spectral overlap is somewhat different in both cases [*cf.* Oevering et al. (1988)]. For the rough comparison of spectral overlaps used here, this difference does not interfere. Therefore, it is not necessary to make assumptions on the mechanism of energy transfer.

[3] If all individual pigments have a similar homogeneous width, then taking into account inhomogeneous broadening has the largest effect on the pigments constituting the broadest Bchl *g* 778 band, diminishing most strongly the overlap between Bchl *g* 778 emission and Bchl *g* 793 absorption.

much shorter delay times. As will be explained in this paragraph, we propose that the bleaching at ~790 nm after a few picoseconds reflects the state $P798^+$ or at least Bchl *g* 793* from which $P798^+$ can be formed efficiently. Whereas the unknown fraction of steady-state $P798^+$ present in our experiments precludes to establish the $P798^+$ quantum yield, it is clear that the rate of charge separation depends on the distribution of the initially populated excited states: the amount of $P798^+$ formed at 50 ps strongly depends on the excitation conditions (Figure 3). Upon excitation at 812 nm, $P798^+$ is formed only on the time scale of ~80 ps (and probably longer, see below). By contrast, upon excitation at 770 nm, the bleaching at ~790 nm is significant after a few picoseconds, when the main (~1.4 ps) phase of the Bchl *g* 793* → Bchl *g* 808* transfer is completed. As mentioned before, this bleaching could in principle reflect some Bchl *g* 793*, which cannot transfer its excitations to Bchl *g* 808 efficiently. However, this is unlikely for the following reasons: (1) no slower Bchl *g* 793* → Bchl *g* 808* transfer phase was identified, (2) there are no indications for more loosely connected Bchl *g* 793 from our room temperature experiments (Liebl et al., 1996), and (3) in 15 K picosecond one-color experiments on membranes of *H. chlorum* in which P798 was completely in the oxidized state prior to the flash, excited Bchl *g* 793 decayed for at least 90% in 2 ps or less (van Noort et al., 1994), whereas in our experiments under excitation at 770 nm at most $\sim^2/_3$ of the bleaching in the Bchl *g* 793 region decayed on this time scale. In fact, the observed ~1.4 ps Bchl *g* 793* → Bchl *g* 808* component in our experiments may in part be due to centers in which P798 cannot be bleached because it is in the oxidized state prior to the flash. We thus suggest that energy is transferred efficiently to P798 from at least a substantial fraction of the excited Bchl *g* 793 pigments, possibly in direct competition with the ~1.4 ps energy transfer to Bchl *g* 808. Because Bchl *g* 793 and P798 both absorb near 790 nm at 20 K, the exact time scale upon which P798 is oxidized in this way cannot be determined from the present experiments, but it can be as fast as a few picoseconds.

Our results strongly indicate that a regime of complete spectral equilibration prior to radical pair formation does not apply for heliobacteria, at least at low temperature, and that the yield of charge separation depends on the excitation wavelength in the time scale of tens of picoseconds. If the yield on the millisecond time scale is excitation wavelength independent, as was reported by Kleinherenbrink et al. (1992), efficient energy transfer from Bchl *g* 808* to P798 must take place in the time scale of hundreds of picoseconds, before Bchl *g** decays to the ground state with its natural lifetime, presumably ~2 ns. We indeed observed additional decay on the 200 ps time scale; the exact determination of its rate constants (>150 ps) is beyond the scope of the present experiments. A strong 200 ps phase in Bchl *g* 808* decay was also observed by van Kan et al. (1989) in *H. chlorum* at 15 K upon picosecond excitation at 532 nm, although we note that in the work by Lin et al. (1994b) in *H. mobilis* at 20 K upon femtosecond excitation at 590 nm most Bchl *g* 808* decayed in 70 ps.

It appears that energy transfer to P798 does not necessarily proceed via Bchl *g* 808*. Therefore, it is unlikely that P798 is surrounded mainly by Bchl *g* 808 pigments (funnel model), as was also concluded from simulations of the trapping process by Lin et al. (1994b). From our observations that Bchl *g* 793* → Bchl *g* 808* energy transfer is relatively slow (as discussed above) and that energy can be efficiently transferred from (some) Bchl *g* 793* to P798, we deduce that if P798 is surrounded by a cluster of similar pigments at all, it is rather by pigments contributing to the Bchl *g* 793 pool. In such a putative "crater" model, once Bchl *g* 808* is formed, energy must be transferred uphill to one of those Bchl *g* 793 pigments prior to trapping. However, as $P798^+$ is efficiently formed from this Bchl *g* 793*, with a yield that is at least comparable to that of energy transfer back to Bchl *g* 808*, this arrangement may lead to more efficient overall trapping. It would be interesting to test this speculative model, which corresponds to an extension of the number of states which forms the effective trap, by numerical simulations.

Energy Transfer to $P798^+$. As $P798^+$ is probably present in a (unknown) fraction of the centers, part of the decay of the signal is likewise due to quenching of the excitations by $P798^+$. Such quenching is expected to be associated with an overall decay of the bleaching signal. In view of the shape of the DAS (Figure 5), we propose that quenching by $P798^+$ is mainly contained in the ~70 ps and the >150 ps components. Van Noort et al. (1994) have tentatively assigned a strong 4 ps decay phase in 15 K picosecond one-color experiments to this process. Although it cannot be excluded that some quenching is also contained in the relatively 2 ps (812 nm excitation) and 7 ps (770 nm excitation) components, we believe that under our experimental conditions the process predominantly takes place on a longer time scale. In this context, we note that Deinum et al. (1991) reported that, at cryogenic temperature, the fluorescence is quenched by a factor of 2 in the presence of $P798^+$. Our assignments can be reconciled with this observation as it is well possible that energy transfer to $P798^+$ occurs faster in all RCs than the slowest decay component of Bchl *g* 808* in the presence of reduced P798, which will dominate the overall fluorescence.

Concluding Remarks. We have spectrally and temporally resolved the processes of spectral equilibration in *H. mobilis*. As expected from simple physical considerations, net uphill energy transfer is not observed at low temperature. Nevertheless, to account for the trapping from excited long-wavelength pigments, even at low temperature, an efficient pathway of uphill energy transfer must exist. For low temperature, random and funnel models for the pigment organization failed to simulate efficient trapping (Lin et al., 1994b). From our experiments, we speculate that a possible "crater-like" model, with P798 surrounded by Bchl *g* 793 pigments, which interestingly may be the only antenna pigments arranged in dimers (van Dorssen et al., 1985, Amesz, 1995), might help to increase the effective cross section of trapping. Future experiments, with more selective excitation of P798, and simulations may test this model.

More generally, we have demonstrated that the yield of oxidation of P on the time scale of tens of picoseconds is dependant on the excitation wavelength, confirming an effect observed less clearly at room temperature (Liebl et al., 1996). It appears obvious from our results that spectral equilibration and trapping cannot be regarded as temporarily separated processes.

REFERENCES

Amesz, J. (1995) in *Anoxygenic Photosynthetic Bacteria* (Blankenship, R. E., Madigan, M. T., & Bauer, C. E., Eds.) pp 687−697, Kluwer, Dordrecht.

Blankenship, R. E. (1994) *Antonie van Leeuwenhoek 65*, 311−329.

Brockmann, H., & Lipinski, A. (1983) *Arch. Microbiol. 136*, 17−19.

Causgrove, T. P., Yang, S., & Struve, W. L. (1989) *J. Phys. Chem. 93*, 6844−6850.

Deinum, G. (1991) Ph.D. Thesis, University of Leiden, The Netherlands.

Deinum, G., Kramer, H., Aartsma, T. J., Kleinherenbrink, F. A. M., & Amesz, J. (1991) *Biochim. Biophys. Acta 1058*, 339−344.

Dexter, D. L. (1952) *J. Chem. Phys. 21*, 836−850.

Du, M., Xie, X., Jia, Y., Mets, L., & Fleming, G. R. (1993) *Chem. Phys. Lett. 201*, 535−542.

Förster, T. (1948) *Ann. Phys. (Leipzig) 2*, 55−75.

Fromme, P., Witt, H. T., Schubert, W.-D., Klukas, O., Saenger, W., & Witt, H. T. (1996) *Biochim. Biophys. Acta 1275*, 76−83.

Haran, G., Wynne, K., Moser, C. C., Dutton, P. L., & Hochstrasser, R. M. (1996) *J. Phys. Chem. 100*, 5562−5569.

Hastings, G., Reed, L. J., Lin, S., & Blankenship, R. E. (1995) *Biophys. J. 69*, 2044−2055.

Hess, S., Chachisvilis, M., Timpmann, K., Jones, M. R., Fowler, G. J. S., Hunter, C. N., & Sundström, V. (1995) *Proc. Natl. Acad. Sci. U.S.A. 92*, 12333−12337.

Jean, J. M., Chan, C.-K., & Fleming, G. R. (1988) *Isr. J. Chem. 28*, 169−175.

Jimenez, R., Dikshit, S. N., Bradforth, S. E., & Fleming, G. R. (1996) *J. Phys. Chem. 100*, 6825−6834.

Jonas, D. M., Lang, M. J., Nagasawa, Y., Joo, T., & Fleming, G. R. (1996) *J. Phys. Chem. 100*, 12660−12673.

Kleinherenbrink, F. A. M., Aartsma, T. J., & Amesz, J. (1991) *Biochim. Biophys. Acta 1057*, 346−352.

Kleinherenbrink, F. A. M., Deinum, G., Otte, S. C. M., Hoff, A. J., & Amesz, J. (1992) *Biochim. Biophys. Acta 1099*, 175−181.

Krauss, N., Hinrichs, W., Witt, I., Fromme, P., Pritzkow, W., Dauter, Z., Betzel, C., Wilson, K. S., Witt, H. T., & Saenger, W. (1993) *Nature 361*, 326−331.

Liebl, U., Rutherford, A. W., & Nitschke, W. (1990) *FEBS Lett. 261*, 427−430.

Liebl, U., Mockensturm-Wilson, M., Trost, J. T., Brune, D. C., Blankenship, R. E., & Vermaas, W. F. J. (1993) *Proc. Natl. Acad. Sci. U.S.A. 90*, 7124−7128.

Liebl, U., Lambry, J.-C., Leibl, W., Breton, J., Martin, J.-L., & Vos, M. H. (1996) *Biochemistry 35*, 9925−9934.

Lin, S., Chiou, H.-C., Kleinherenbrink, F. A. M., & Blankenship, R. E. (1994a) *Biophys. J. 66*, 437−445.

Lin, S., Kleinherenbrink, F. A. M., Chiou, H.-C., & Blankenship, R. E. (1994b) *Biophys. J. 67*, 2479−2489.

Monshouwer, R., Ortiz de Zarate, I., van Mourik, F., & van Grondelle, R. (1995) *Chem. Phys. Lett. 246*, 341−346.

Nitschke, W., Sétif, P., Liebl, U., Feiler, U., & Rutherford, A. W. (1990) *Biochemistry 29*, 11079−11088.

Oevering, H., Verhoeven, J. W., Paddon-Row, M. N., Cotsaris, E., & Hush, N. S. (1988) *Chem. Phys. Lett. 143*, 488−495.

Press, W. H., Flannery, B. P., Teukolsky, S. A., & Vetterling, W. T. (1989) *Numerical Recipes*, Cambridge University Press, New York.

Savikhin, S., & Struve, W. S. (1994) *Biochemistry 33*, 11200−11208.

Shiozawa, J. A., Alberte, R. S., & Thornber, J. P. (1974) *Arch. Biochem. Biophys. 165*, 388−397.

Smit, H. W. J., van Dorssen, R. J., & Amesz, J. (1989) *Biochim. Biophys. Acta 973*, 212−219.

Stanley, R. J., King, B., & Boxer, S. G. (1996) *J. Phys. Chem. 100*, 12052−12059.

Trissl, H.-W. (1993) *Photosynth. Res. 35*, 247−263.

Trost, J. T., & Blankenship, R. E. (1989) *Biochemistry 28*, 9898−9904.

van de Meent, E. J., Kleinherenbrink, F. A. M., & Amesz, J. (1991) *Biochim. Biophys. Acta 1015*, 223−230.

van de Meent, E. J., Kobayashi, M., Erkelens, C., van Veelen, P. A., & Amesz, J. (1992) *Biochim. Biophys. Acta 1058*, 356−362.

van der Lee, J., Bald, D., Kwa, S. L. S., van Grondelle, R., Rögner, M., & Dekker, J. P. (1993) *Photosynth. Res. 35*, 311−321.

van Dorssen, R. J., Vasmel, H., & Amesz, J. (1985) *Biochim. Biophys. Acta 809*, 199−203.

van Grondelle, R., Dekker, J. P., Gillbro, T., & Sundström, V. (1994) *Biochim. Biophys. Acta 1187*, 1−65.

van Kan, P. J. M., Aartsma, T. J., & Amesz, J. (1989) *Photosynth. Res. 22*, 22−68.

van Noort, P. I., Aartsma, T. J., & Amesz, J. (1992) *Biochim. Biophys. Acta 1140*, 15−21.

van Noort, P. I., Aartsma, T. J., & Amesz, J. (1994) *Biochim. Biophys. Acta 1184*, 21−27.

Vasmel, H., Swarthoff, T., Kramer, H. J. M., & Amesz, J. (1983) *Biochim. Biophys. Acta 725*, 361−367.

Vos, M. H., Klaassen, H. E., & van Gorkom, H. J. (1989) *Biochim. Biophys. Acta 973*, 163−169.

Vos, M. H., Jones, M. R., Breton, J., Lambry, J.-C., & Martin, J.-L. (1996) in *Ultrafast Phenomena X* (Barbara, P. F., Fujimoto, J. G., Knox, W. H., & Zinth, W., Eds.) pp 332−333, Springer-Verlag, Berlin.

White, N. T. H., Beddard, G. S., Thorne, J. R. G., Feehan, T. M., Keyes, T. E., & Heathcote, P. (1996) *J. Phys. Chem. 100*, 12086−12099.

BI9625197